IEICE TRANS. FUNDAMENTALS, VOL.E92–A, NO.2 FEBRUARY 2009

PAPER Special Section on Analog Circuit Techniques and Related Topics

Technique to Improve the Performance of Time-Interleaved A-D Converters with Mismatches of Non-linearity

Koji ASAMI[†a)], ***Member***, **Takahide SUZUKI**[††], **Hiroyuki MIYAJIMA**[††], **Tetsuya TAURA**[††], ***Nonmembers***, ***and*** **Haruo KOBAYASHI**[††b)], ***Member***

SUMMARY One method for achieving high-speed waveform digitizing uses time-interleaved A-D Converters (ADCs). It is known that, in this method, using multiple ADCs enables sampling at a rate higher than the sampling rate of the ADC being used. Degradation of the dynamic range, however, results from such factors as phase error in the sampling clock applied to the ADC, and mismatched frequency characteristics among the individual ADCs. This paper describes a method for correcting these mismatches using a digital signal processing (DSP) technique for automatic test equipment applications. This method can be applied to any number of interleaved ADCs, and it does not require any additional hardware; good correction and improved accuracy can be obtained simply by adding a little to the computing overhead.

key words: *time-interleaved A-D converters, non-linearity, foreground calibration, digital error correction, automatic test equipment*

1. Introduction

In recent times, as digital communication has gotten faster, A-D converters (ADCs) have been increasingly demanded in instruments and Automatic Test Equipments (ATEs) for evaluating such signals. For example, in a UWB communication system [1], a Gsps-order ADC is required in order to measure a signal with a 500 MHz bandwidth. Time-interleaved AD conversion is one method of achieving AD conversion with a higher sampling rate [2]. In this method, multiple ADCs are combined to achieve the equivalent of an increased sampling rate. Figure 1 shows an example of 4 channel interleaved ADC system. Mismatched frequency characteristics including the sampling clock timing error in the channel ADCs used, however, are known to lead to the occurrence of false spurious signals [3], [4]. These mismatches can be analyzed as linear mismatches.

A number of correction methods for linear mismatches have been proposed in other papers [4]–[8]. However, these methods do not consider non-linear mismatches for the interleaved ADCs. Since the non-linear mismatches of each A-to-D channel also influence the degradation of the dynamic range, they should also be considered in the interleaved ADC, for example the DC non-linearity. The influence of the interleaved ADC on the non-linear mismatches has been reported in [9].

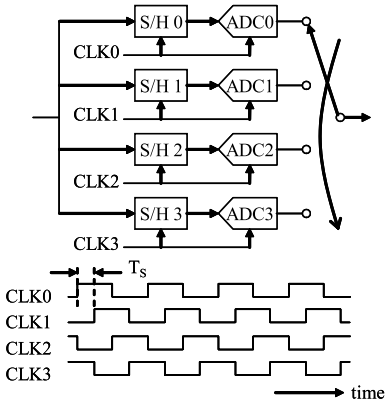

Fig. 1 4-channel time-interleaved ADC.

This paper analyzes the behavior of the non-linear mismatches mathematically and constructs a model of the spurious signal occurrences caused by the mismatches. Based on the model, this paper proposes a compensation method for both linear and non-linear mismatches using only post-AD-conversion digital signal processing.

First, this paper describes a mathematical model of the interleaved AD conversion, and an analysis of spurious occurrences caused by any mismatches. It then discusses the compensation method itself, and provides an actual signal processing algorithm.

The proposed method is targeted for ATE applications, and it may be difficult to apply directly to consumer electronics applications (such as cellular phones) because signal sources are required to identify the characteristics of each channel ADC; the ATE has signal sources inside. Also it is classified as a foreground digital calibration algorithm.

2. Time-Interleaved AD Conversion Method

This section uses mathematical expressions to describe the behavior of the interleaved ADCs. AD conversion incorporates two functions: quantization and sampling. As quantization is largely irrelevant to this paper, voltage is treated as a continuous quantity. The time dimension is also treated as a continuous quantity, while sampling is expressed using a delta function. In other words, sampling of the input signal waveform $x(t)$ to be measured with the sampling period Ts

Manuscript received June 16, 2008.
Manuscript revised September 9, 2008.

[†]The author is with Advantest Corporation, Gunma R&D Center, Gunma-ken, 370-0718 Japan.
[††]The authors are with Electronic Engineering Department, Graduate School of Engineering, Gunma University, Kiryu-shi, 376-8515 Japan.
a) E-mail: koji.asami@jp.advantest.com
b) E-mail: k_haruo@el.gunma-u.ac.jp

DOI: 10.1587/transfun.E92.A.374

can be expressed as follows:

$$\overline{x}(t) = x(t) \cdot \sum_{n=-\infty}^{\infty} \delta(t - n \cdot T_s) = \sum_{n=-\infty}^{\infty} x(nT_s) \cdot \delta(t - n \cdot T_s). \quad (1)$$

Here, $\delta(t)$ is the delta function. Fourier transform of the equation in (1) results in:

$$\overline{X}(f) = X(f) * \sum_{n=-\infty}^{\infty} \delta\left(f - \frac{n}{T_s}\right) = \sum_{n=-\infty}^{\infty} X\left(f - \frac{n}{T_s}\right) \quad (2)$$

where, $X(f)$ represents the Fourier transform of $x(t)$. This equation shows periodicity occurring as the result of sampling the input signal spectrum. According to the sampling theorem, aliasing does not occur at this point so long as the single-sided spectrum of $x(t)$ is 1/2 of the sampling frequency or less.

Next, sampling for this period Ts is achieved using M-channel interleaved ADCs. First, the sampling clock is distributed into M sampling clocks. Each of the M clocks can be expressed mathematically as:

$$P_m(t) = \sum_{n=-\infty}^{\infty} \delta(t - (M \cdot n + m) \cdot T_s) \quad (m = 0, 1, \cdots, M-1). \quad (3)$$

Fourier transform of Eq. (3) results in:

$$P_m(f) = e^{-j2\pi f(mT_s)} \frac{1}{M \cdot T_S} \sum_{k=-\infty}^{\infty} \delta\left(f - \frac{k}{M \cdot T_S}\right) = \frac{1}{M \cdot T_S} \sum_{k=-\infty}^{\infty} \delta\left(f - \frac{k}{M \cdot T_S}\right) e^{-j2\pi km/M} \quad (m = 0, 1, \cdots, M-1). \quad (4)$$

The result of sampling input signal waveform $x(t)$ using each of these clocks can be expressed:

$$X_m(f) = \frac{1}{M \cdot T_S} \sum_{k=-\infty}^{\infty} X\left(f - \frac{k}{M \cdot T_S}\right) e^{-j2\pi km/M} \quad (m = 0, 1, \cdots, M-1). \quad (5)$$

This equation shows the spectrum replicas of the original spectrum occur at every integral multiple of $1/(MT_S)$. The replicas, except M times $1/(MT_S)$, are eliminated by linear addition of the frequency characteristics. That is to say:

$$X(f) = \sum_{m=0}^{M-1} X_m(f) = \frac{1}{T_S} \sum_{k=-\infty}^{\infty} X\left(f - \frac{k}{T_S}\right). \quad (6)$$

This equation shows the interleaving method is successful.

3. Analysis of Non-linear Mismatch Effects in Time-Interleaved ADCs

The previous section described the achievement of an ADC of M times the individual ADC sampling rate using M channel interleaved ADCs. This section considers cases in which the non-linear characteristics vary among the ADCs. The effects of linear mismatches, which means mismatches of the frequency characteristics including the clock skew, have been discussed in [4].

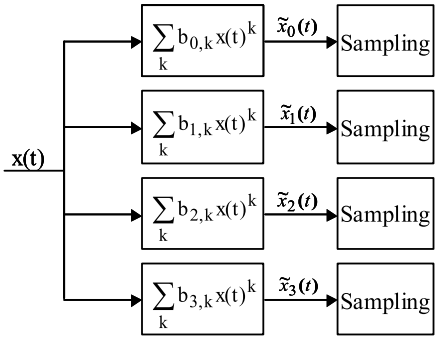

Fig. 2 Non-linear mismatch model of time interleaved ADCs.

First, when the input waveform is defined as $x(t)$, the non-linear characteristic of the m-th ADC is defined as:

$$\tilde{x}_m(t) = \sum_q b_{m,q} x(t)^q \quad (7)$$

where, q is the order of the non-linear distortion. Figure 2 shows the model of 4-channel interleaving with non-linear characteristics. This non-linear signal is sampled by an ideal ADC, and the Fourier transform of the signal sampled by the m-th ADC can be expressed as:

$$\overline{X}_m(f) = \frac{1}{M \cdot T_S} \sum_{k=-\infty}^{\infty} \tilde{X}_m\left(f - \frac{k}{M \cdot T_S}\right) e^{-j2\pi km/M} \quad (8)$$

where, $\tilde{X}_m(f)$ represents the Fourier transform of $\tilde{x}_m(T)$. If the non-linear characteristics of ADCs are matched between interleaved channels, that is to say:

$$\tilde{x}_0(t) = \tilde{x}_1(t) = \cdots = \tilde{x}_{M-1}(t) \equiv \tilde{x}(t) \quad (9)$$

the frequency spectrum can be expressed as follows:

$$\tilde{X}_0(f) = \tilde{X}_1(f) = \cdots = \tilde{X}_{M-1}(f) \equiv \tilde{X}(f). \quad (10)$$

As a result, the interleaved data can eventuate Eq. (6), and it can be expressed as:

$$\overline{X}(f) = \sum_{m=0}^{M-1} \overline{X}_m(f) = \frac{1}{T_S} \sum_{k=-\infty}^{\infty} \tilde{X}\left(f - \frac{k}{T_S}\right). \quad (11)$$

On the other hand, if the characteristics of the ADCs do not satisfy Eq. (9), the interleaved data is expressed as:

$$\overline{X}(f) = \frac{1}{M \cdot T_S} \sum_{k=-\infty}^{\infty} \sum_{m=0}^{M-1} \tilde{X}_m\left(f - \frac{k}{M \cdot T_S}\right) e^{-j2\pi km/M}. \quad (12)$$

This equation shows the spectrum replica appear at any whole multiple k of $\frac{1}{MT_S}$. This means that the spectrum replica occur in every integral multiple of $\frac{1}{MT_S}$.

4. Compensation Algorithm

Although ADC non-linear characteristics can be considered either as a DC non-linearity or an AC non-linearity, it has been reported that the performance can be improved by correction of only the DC non-linearity [10]. Therefore, we consider the DC non-linearity here, especially INL (Integral Non-Linearity). Figure 3(b) shows a model of an ADC with frequency characteristic and INL. They can be measured using a signal generator in the ATE. Since only one analog front-end circuit is set in front of the interleaved ADCs, this case is available. Since DC non-linearity influences only gain as shown in Fig. 3(a) in general, in Eq. (7) is a real number coefficient. The mathematical model of this case can be expressed as:

$$\overline{X'}(f) = \frac{1}{M \cdot T_S} \sum_{k=-\infty}^{\infty} \sum_{m=0}^{M-1} F_{INL}^{m}\left(A_m\left(f - \frac{k}{M \cdot T_S}\right) X_m\left(f - \frac{k}{M \cdot T_S}\right)\right) e^{-j2\pi mk/M} \quad (13)$$

where, F_{INL}^{m} is a function which represents the INL of m-th A-to-D channel in the frequency domain, and Am represents the frequency characteristic of the m-th A-to-D channel. Based on Eq. (13), the compensation algorithm is constructed.

The compensation of the INL can be accomplished by multiplying by the inverse function $(F_{INL}^{m})^{-1}$ in Eq. (13). As a result, Eq. (13) is rewritten as

$$X'(f) = \frac{1}{M \cdot T_S} \sum_{k=-\infty}^{\infty} \sum_{m=0}^{M-1} A_m\left(f - \frac{k}{M \cdot T_S}\right) X_m\left(f - \frac{k}{M \cdot T_S}\right) e^{-j2\pi mk/M}. \quad (14)$$

This equation includes only frequency characteristics mismatches, and a compensation method for these mismatches has been reported in [4].

Figure 4 shows the compensation flow chart. Based on the aforesaid models, the compensations of INL mismatches and frequency characteristic mismatches are carried out serially. To compensate the INL, the inverse function is made into a table for each ADC individually. On the other hand, the algorithm for the correction of the frequency mismatches can be performed for the whole interleaved ADC system, not by individual ADC. The INL characteristics are measured in advance, and the inverse functions of the characteristics are calculated algorithmically, for example using a non-linear programming method.

As an alternative, the distortion components can be canceled from the ADC output data using the identified polynomial coefficients in Eq. (7). In LSI testing, since the measured waveforms are mostly known and the sinusoidal waveforms are often used, it is easy to compensate the distortion. If the non-linear characteristics include any phase distortion due to analog circuits, besides INL, the $b_{m,k}$ become complex numbers, and the inverse function $(F_{INL}^{m})^{-1}$ is also a complex numbered function.

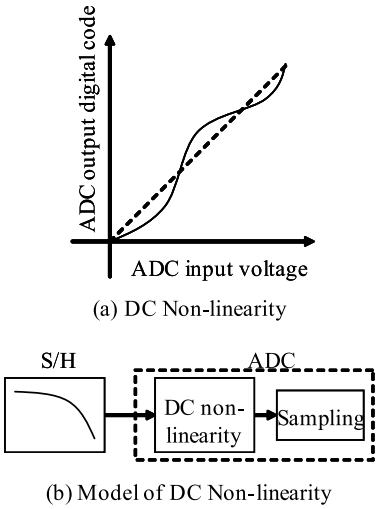

Fig. 3 Model of DC non-linearity case.

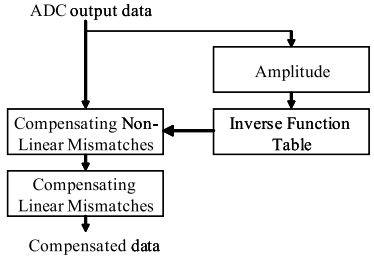

Fig. 4 Compensation flow chart.

5. Simulation

To confirm the validity of the compensation algorithm, we performed a computer simulation. First, we set the non-linearity and frequency characteristics for each ADC as shown in Fig. 5. We digitized a sinusoidal waveform using the 4-channel interleaved ADCs with mismatches. A random noises of SNR = 85 dB was added as the quantization noise. In this simulation, we assume that the effective number of bits for the ADC is about 14 bits, and its quantization noise is substituted by a white noise. The input signal frequency was set to 81 under the sampling rate of 16384. Figure 6(a) shows the spectra of the interleaved ADC with the mismatches. Many spurious components due to the mismatches are observed besides distortion components. Figure 6(b) shows the results of only non-linear mismatch correction. Although harmonics and spurious components due to non-linear mismatches are eliminated, spurious of linear mismatches remain. Finally, we compensate both non-linear and linear mismatches. The spurious occurrences can be seen to have disappeared completely, as shown in Fig. 6(c).

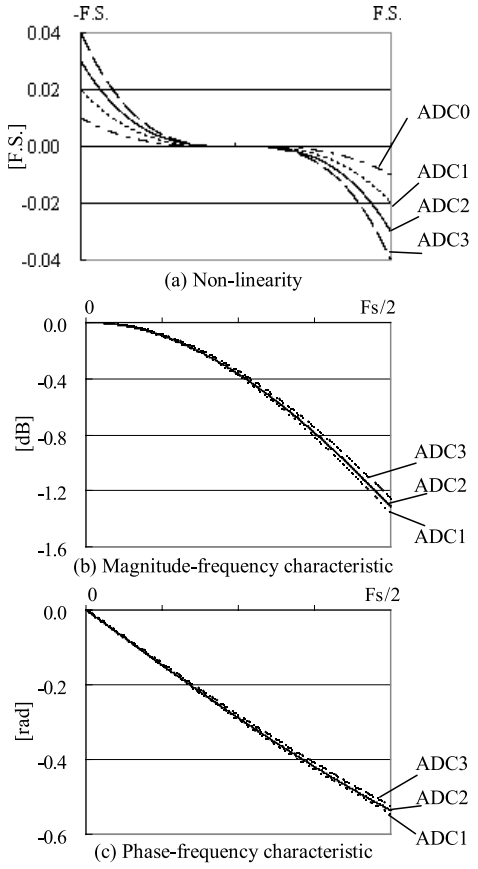

Fig. 5 Simulation system.

6. Performance of the Compensation Technique

The measurement accuracy of the non-linearity of the ADCs that are being corrected affects the compensation results. It is difficult to characterize this analytically, but the amount of error can be investigated by simulation. As an example, the compensation error is simulated for the case of 4 interleaved ADCs where only one ADC is measured incorrectly. That is, initially, all the characteristics of the ADCs are identical and there is no need for compensation. Then the value of the INL of only one of the ADCs is adjusted with a simulated error ranging from 10% to .01%, the compensation operation is carried out, and the resulting SFDR (spurious free dynamic range) is computed. The INL is assumed as only 3rd order:

$$\tilde{x}(t) = x(t) + b_3 \cdot x(t)^3 \tag{15}$$

and b_3 is expressed as a percentage of the FS (Full Scale) range. Table 1 shows the resulting SFDR [dBc] for various percentages, and Fig. 7 shows the spectrum with 0.1% error.

The relation between SNR and the effective number of bits is well known as SNR = 6.02 × (number of bits) + 1.76 [dB]. To secure a SNR equivalent to 12 bit accuracy under this condition, it is necessary to measure the INL of the ADC to 0.1% accuracy or better.

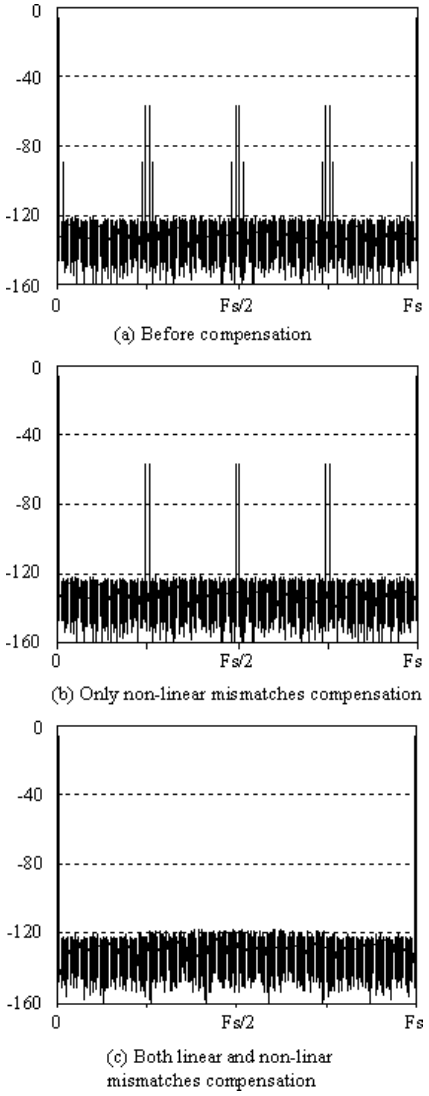

Fig. 6 Simulation results of 1-tone input.

Table 1 Simulation results for the performance of the compensation technique.

3rdDist[FS]	SFDR[dBc]
0.1	- 31
0.01	- 51
0.001	- 71
0.0001	- 91

7. Experimental Results

The proposed model and algorithm have been experimentally evaluated with four-channel interleaved ADCs. They are composed of 16-bit ADCs from the market. A 39.99023438 MHz (=819/4096*200 MHz) sinusoidal wave is generated by the signal generator, and it is sampled by the interleaved ADCs at 200 Msps. Figure 9(a) shows the frequency domain data calculated by the FFT. In this case, SNDR (signal to noise and distortion ratio) was calculated as 52.5 dB. Spurious components appear due to the mis-

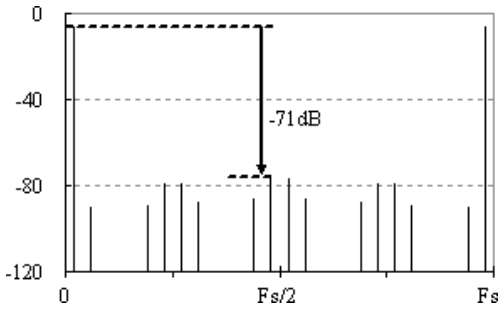

Fig. 7 Sprious with the compensation error of 0.1%.

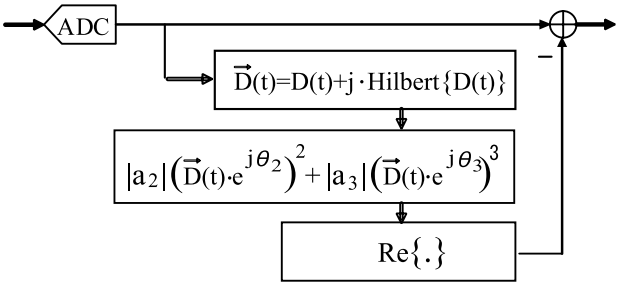

Fig. 8 Block diagram for non-linear compensation.

matches of the ADC channels. The triangle marks show the spurious components due to the non-linear mismatches, and their level is 64.5 dBc. From the position of these spurious components, they can be shown to be second harmonic distortion. Therefore, we have assumed that it has been enough to consider only the second and the third order coefficients for the polynomial equation with 0 dB linear gain. When a cosine wave of the frequency f_0 is input to such non-linear model, the distorted signal is expressed as:

$$
\begin{aligned}
&A \cdot \cos(2\pi f_0 t + \phi) + \sum_{k=2}^{3} |a_k| \cdot (A \cdot \cos(2\pi f_0 t + \phi + \theta_k))^k \\
&= A^2 \cdot \frac{|a_2|}{2} \\
&+A \cdot \left(\cos(2\pi f_0 t + \phi) + \frac{3}{4} \cdot A^2 \cdot |a_3| \cos(2\pi f_0 t + \phi + \theta_3) \right) \\
&+A^2 \cdot \frac{|a_2|}{2} \cdot \cos(2\pi \cdot 2 f_0 t + 2\phi + 2\theta_2) \\
&+A^3 \cdot \frac{|a_3|}{4} \cdot \cos(2\pi \cdot 3 f_0 t + 3\phi + 3\theta_3) \qquad (16)
\end{aligned}
$$

where, 'A' and 'ϕ' represent the amplitude and the initial phase of the cosine wave respectively, and $|a_k|$ and θ_k represent the gain and the phase rotation of the non-linear characteristics respectively. Based on the relation expressed with the equation, the non-linear coefficients are calculated by analyzing the frequency spectrum of the harmonics as shown in Table 2. In this experiment, since the distortion due to the third order is small enough compared to the fundamental wave spectrum, the component turned up to the fundamental spectrum among the third order distortion was disregarded. In general, if the third order distortion is large,

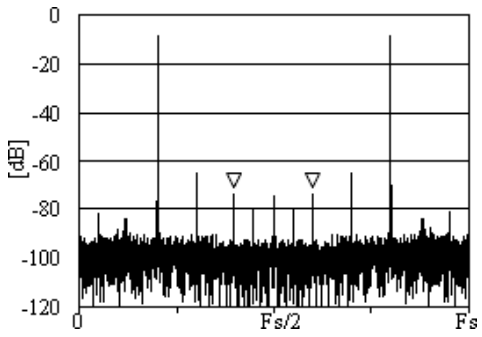

(a) Before compensation.

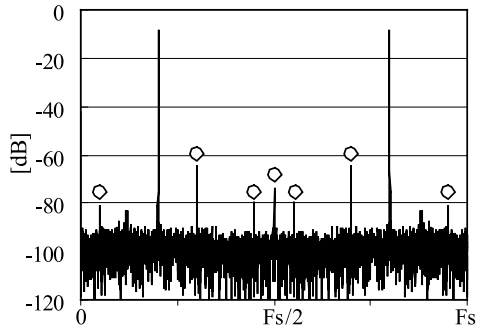

(b) Only non-linear mismatches compensation.

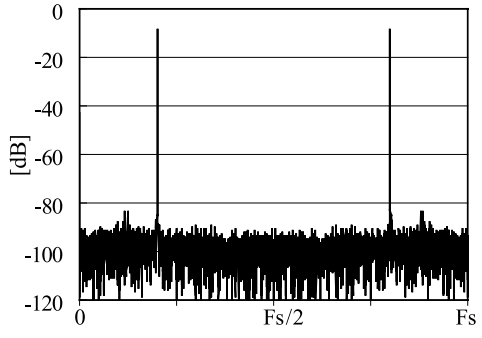

(c) Both non-linear and linear mismatches compensation.

Fig. 9 Experimental results.

Table 2 Identification result of distortion.

	2nd order		3rd order	
	Gain	Phase[rad]	Gain	Phase[rad]
ADC0	0.0017	-1.4690	0.0012	0.9818
ADC1	0.0015	-1.3968	0.0009	-0.9995
ADC2	0.0018	-1.3841	0.0008	0.9932
ADC3	0.0015	-1.3567	0.0005	-0.8508

it is required to be subtracted from the fundamental wave component.

In addition, if there are some higher order distortions, we have to identify which Nyquist region they are in. This means that the harmonics components we analyze should be distinguished from the image components by the sampling.

Then, the captured signal is compensated by applying these values to the compensation algorithm as shown in

Fig. 8. In this experiment, the algorithm substitutes for the compensation by the inverse function. To rotate the phases, the captured signal is converted into the complex number by Hilbert transform. Then, it is squared and tripled, and multiplied by the gain of the coefficients. The compensation results are shown in Fig. 9(b). The spurious components due to the non-linear mismatches are suppressed.

The circle marks in Fig. 9(b) show the spurious signals due to the linear mismatches of the interleaved ADCs, and the maximum one is 56.2 dBc. We have also compensated the linear mismatches, and the result is shown in Fig. 9(c). The spurious components can be suppressed. In this compensation, SNDR was calculated as 55.7 dB and the maximum level of the spurious component is 75.1 dBc. That is to say, SNDR was improved by only 3 dB, but SFDR (spurious free dynamic range) was improved by 18.9 dB. Thus, it has been confirmed that the non-linear and linear mismatches can be compensated individually.

8. Conclusion

We have developed a mathematical model for interleaved ADC channels including both linear and non-linear mismatches. The linear mismatches include the frequency characteristics and the misalignment of the sampling instances, and the non-linear mismatches include the INL of the individual ADC. Based on the model, we have proposed a compensation technique using a DSP algorithm for ATE applications. It makes possible a major improvement to spurious-free dynamic range by correcting both linear and non-linear mismatches of the respective ADCs through post conversion digital signal processing. The advantages of this technique are that it requires no additional hardware, and that it consumes only slight computation overhead. This technique can be applied even if there is a change to the number of interleaved ADCs.

References

[1] http://wimedia.org/en/
[2] W.C. Black, Jr. and D.A. Hodges, "Time interleaved converter arrays," IEEE J. Solid-State Circuits, vol.15, pp.1022–1029, Dec. 1980.
[3] N. Kurosawa, H. Kobayashi, K. Maruyama, H. Sugawara, and K. Kobayashi, "Explicit analysis of channel mismatch effects in time-interleaved ADC systems," IEEE Trans. Circuits Syst. I, vol.48, no.3, pp.261–271, March 2001.
[4] K. Asami, "An algorithm to improve the performance of M-channel time-interleaved A-D converters," IEICE Trans. Fundamentals, vol.E90-A, no.12, pp.2846–2852, Dec. 2007.
[5] H. Jin and E.K. F. Lee, "A digital-background calibration technique for minimizing timing-error effects in time-interleaved ADCs," IEEE Trans. Circuits Syst. II, vol.47, no.7, pp.603–613, July 2000.
[6] K. Poulton, R. Neff, A. Muto, W. Liu, A. Burstein, and M. Heshami, "A 4 Gsample/s 8 b ADC in 0.35 μm CMOS," ISSCC Digest of Technical Papers, pp.126–434, Feb. 2002.
[7] P. Schvan, J. Bach, C. Falt, P. Flemke, R. Gibbins, Y. Greshishchev, N. Ben-Hamida, D. Pollex, J. Sitch, S.-C. Wang, and J. Molczarsk, "A 24 GS/s 6 b ADC in 90 mm CMOS," ISSCC Digest of Technical Papers, pp.544–545, Feb. 2008.
[8] S.R. Velazquez, T.Q. Nguyen, S.R. Broadstone, and J.K. Roberge, "A hybrid filter bank approach to analog-to-digital conversion," Proc. IEEE-SP Int. Symp. Time-Frequency Time-Scale Anl., pp.116–119, Oct. 1994.
[9] N. Kurosawa, H. Kobayashi, and K. Kobayashi, "Channel linearity mismatch effects in time-interleaved ADC systems," IEICE Trans. Fundamentals, vol.E85-A, no.4, pp.749–756, April 2002.
[10] T. Komuro, S. Sobukawa, H. Sakayori, M. Kono, and H. Kobayashi, "Total harmonic distortion measurement system for electronic devices up to 100 MHz with remarkable sensitivity," IEEE Trans. Instrum. Meas., vol.56, no.6, pp.2360–2368, Dec. 2007.

Koji Asami received the M.E. degree in electronics from Gunma University in 1991. Since 1991, he has been with ADVANTEST corporation, Gunma R&D Center, Japan, where he has been engaged in researching the signal processing technique to test mixed-signal LSIs. Currently he is also pursuing the Ph.D. degree at Gunma University.

Takahide Suzuki received the B.S. degree in electronic engineering from Gunma University in 2007, and currently he is a graduate student in master course there. His research interests includes electronic measurement technology.

Hiroyuki Miyajima received the B.S. degree in electronic engineering from Gunma University in 2008, and currently he is a graduate student in master course there. This research interests include analog integrated circuit design and digital signal processing.

Tetsuya Taura received the B.S. and M.S. degrees in electronic engineering from Gunma University in 2006 and 2008 respectively. He is currently working for Tohoku Electric Power Co., Inc.

Haruo Kobayashi received the B.S. and M.S. degrees in information physics from University of Tokyo in 1980 and 1982 respectively, the M.S. degree in electrical engineering from University of California at Los Angeles (UCLA) in 1989, and the Dr.Eng. degree in electrical engineering from Waseda University in 1995. He joined Yokogawa Electric Corp. Tokyo, Japan in 1982, where he was engaged in the research and development related to measuring instruments and mini-supercomputers. From 1994 to 1997, he was involved in research and development of ultra-high-speed ADCs/DACs at Teratec Corp. In 1997 he joined Gunma University and presently is a Professor in Electronic Engineering Department there. He was also an adjunct lecturer at Waseda University from 1994 to 1997. His research interests include mixed-signal integrated circuits design and signal processing algorithms. He received Yokoyama Award in Science and Technology in 2003, and the Best Paper Award from the Japanese Neural Network Society in 1994.